Measurement of the Tip and Friction Force Acting on a Needle during Penetration

Hiroyuki Kataoka[1], Toshikatsu Washio[1], Kiyoyuki Chinzei[1],
Kazuyuki Mizuhara[2], Christina Simone[3], and Allison M. Okamura[3]

[1] National Institute of Advanced Industrial Science and Technology,
1-2 Namiki, Tsukuba-shi, Ibaraki, 305-8564 Japan
gacha@ni.aist.go.jp, washio.t@aist.go.jp, k.chinzei@aist.go.jp
[2] Dept. of Mechanical Engineering, Tokyo Denki University,
2-2 Nishiki-cho, Kanda, Chiyoda-ku, Tokyo, 101-8457 Japan
mizuhara@cck.dendai.ac.jp
[3] Dept. of Mechanical Engineering, Johns Hopkins University,
322 New Engineering Building, 3400 N. Charles Street, Baltimore, MD 21218, USA
csimone@titan.me.jhu.edu, aokamura@jhu.edu

Abstract. We present the tip and friction forces acting on a needle during penetration into a canine prostate, independently measured by a 7-axis load cell newly developed for this purpose. This experimental apparatus clarifies the mechanics of needle penetration, potentially improving the development of surgical simulations. The behavior of both tip and friction forces can be used to determine the mechanical characteristics of the prostate tissue upon penetration, and the detection of the surface puncture, which appears in the friction force, makes it possible to estimate the true insertion depth of the needle in the tissue. The friction model caused by the clamping force on the needle can also be determined from the measured friction forces.

1 Introduction

Needle insertion is a basic and least invasive method of treatment. However, surgeons must possess considerable skill and experience in order to control the needle path so that the needle may reach a preoperatively determined target inside the tissue. Because thin needles can deflect inside the tissue, and the tissue can also deform, surgeons must predict these deflections and deformations. Since surgeons commonly predict such behavior by feeling the force acting on the needle with their fingers, it is important to train realistic insertion tasks using a force-feedback needle simulator.

In order to simulate the forces acting on a needle, the mechanism of force generation should be clarified and modeled. Considering that the needle shaft rubs against the tissue while the needle tip cuts the tissue, the force on the needle shaft should be distinguished from that on the needle tip. Following this idea, we assumed three different forces acting on the needle as shown in Fig.1: the tip force acting on the needle tip in the axial direction, the friction force acting on the side wall of the needle shaft in the axial direction, and the clamping force acting on the side wall of the needle shaft in the normal direction. The tip force concerns the cutting force when the needle

T. Dohi and R. Kikinis (Eds.): MICCAI 2002, LNCS 2488, pp. 216–223, 2002.

is penetrating the tissue, and its magnitude is affected by the shape of the tip of the needle. The Coulomb friction force is defined as the scalar product of the normal force acting on the surface and the coefficient of friction. Viscous friction, the product of a damping coefficient and relative velocity of the two materials, can also affect the total friction force. In the case of the needle, the normal force is determined as the total amount of clamping force. When the needle is inserted into the tissue, the clamping force increases due to the increase of the contact area between the needle and the tissue. The clamping force is the resistance force of the tissue compressed out from the needle path, which is affected by the incision shape in the tissue created by the needle tip, as well as the needle gauge.

The total axial force of the needle is the sum of the tip force and the friction force. Some researchers reported the total axial force of the needle. Hiemenz, et al. [1] and Westbrook, et al. [2] detected the puncture of ligamentum flavum or dura by the peak in the total axial force measured on the penetration. Brett, et al. [3-4] also measured and modeled the total axial force to identify the tissue type on the needle path on spinal anesthesia. All of them measured the total axial force acting on the needle, but did not separate the tip and friction force from the total axial force. Therefore, their data were insufficient to quantify each force even though Brett referred to the friction force in his model. Simone and Okamura [5] separated cutting and friction forces in experiments with liver tissue, but did not measure them simultaneously.

In this study, we independently quantified the tip and friction forces of a needle on penetration with a load cell newly developed for this purpose. Since we are considering the needle simulator of brachytherapy for the prostate, we inserted needles into the prostate of a canine cadaver, and investigated the mechanism of the generation of the tip and friction forces according to the experimental data.

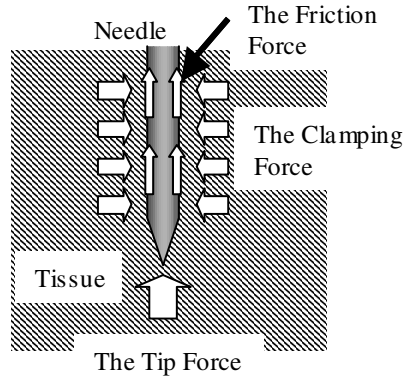

Fig. 1. The forces acting on a needle in tissue

2 Materials and Methods

In order to independently measure the tip and friction forces acting on a needle, a load cell named 7-axis load cell was developed. Figure 2 shows the structure of the 7-axis load cell, and Fig.3 shows the prototype used in the experiments. This load cell consists of an inner needle of 1.15mm diameter with a triangular pyramid tip and a cylindrical outer needle of 1.4mm diameter (similar to biopsy needles). The outer needle is

attached to the load cell casing via a 6-axis load cell, and the inner needle is attached to the outer needle via a 1-axis load cell. Since only the tip of the inner needle appears outside the outer needle, the 1-axis load cell outputs the tip force of the inner needle. The 6-axis load cell outputs the total force and torque acting on the both needles. The load capacity of the 7-axis load cell is shown in Table 1. The tip force of this system is measured as the tip force of the inner needle, and the friction force is calculated by subtracting the tip force from the axial force component of the output of the 6-axis load cell.

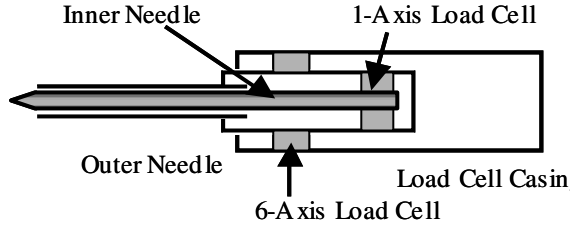

Fig. 2. Structure of the 7-axis load cell

Fig. 3. Picture of the 7-axis load cell

Table 1. Maximum load capacity of the 7-axis load cell

Axis	Maximum Load Capacity
Fx, Fy	20N
Fz	50N
Ftip	10N (for measurement)
Tx, Ty	2Nm
Tz	0.3Nm

A fresh beagle cadaver (31kg weight) was prepared and frozen for 2 weeks until the experiment. After 3 days defrosting, it was laid supine on the operating table and the abdomen was opened to expose the prostate. The 7-axis load cell with a set of needles was attached on a linear stage above the prostate, and driven vertically at a constant speed of 2.95mm/sec. Figure 4 shows the experimental apparatus.

In our penetration procedure, the needle was first positioned 5mm above the surface of the prostate, driven down 25mm, then stopped and remained still in the prostate for 5sec. Finally, the needle was pulled up 20mm. Data from the 7-axis load cell were recorded at a 50Hz sampling rate, together with the trigger signal of the linear stage controller, by a PC computer. The data was analyzed after the experiment. The

penetration was performed twice, changing the puncture positions on the prostate surface to prevent the needle from going into the hole created by the previous penetration. The motion of the needle in the cadaver was monitored by a biplane X-ray system during the penetration.

The total amount of the clamping force increases following the increase of the insertion depth of the needle in the prostate. Since the prostate surface is commonly compressed by the needle before its puncture, the true insertion depth of the needle was estimated by subtracting the compressed depth of the prostate surface from the driving distance of the needle by the linear stage.

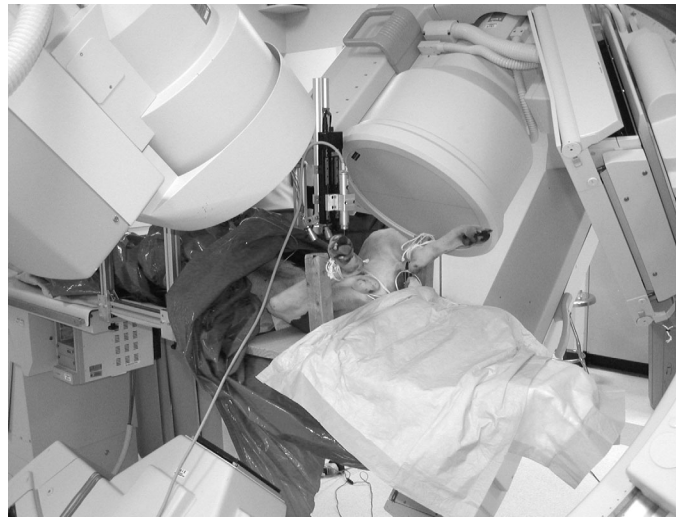

Fig. 4. Overview of the experimental apparatus with a canine cadaver. The tubes above the canine are part of the biplane X-ray system used to monitor the motion of the needle in the canine

3 Results

Figure 5 shows the forces acting on the needle and the position of the needle tip versus time during penetration into the canine prostate. Each force data point was plotted from an average five samples. The step line in the force plot is the trigger signal of the linear stage controller, and the position of the needle tip is plotted according to this signal. The thick lines indicate the total axial forces. The dotted lines indicate the tip forces. The thin lines indicate the friction forces calculated by subtracting the tip forces from the corresponding total axial forces.

The position of the needle tip is presented as 0mm at the prostate surface before the penetration, and positive in the insertion direction. The needle tip positioned at -5mm at the beginning, and touched the prostate surface about at 1.7sec. We defined this period as (A).

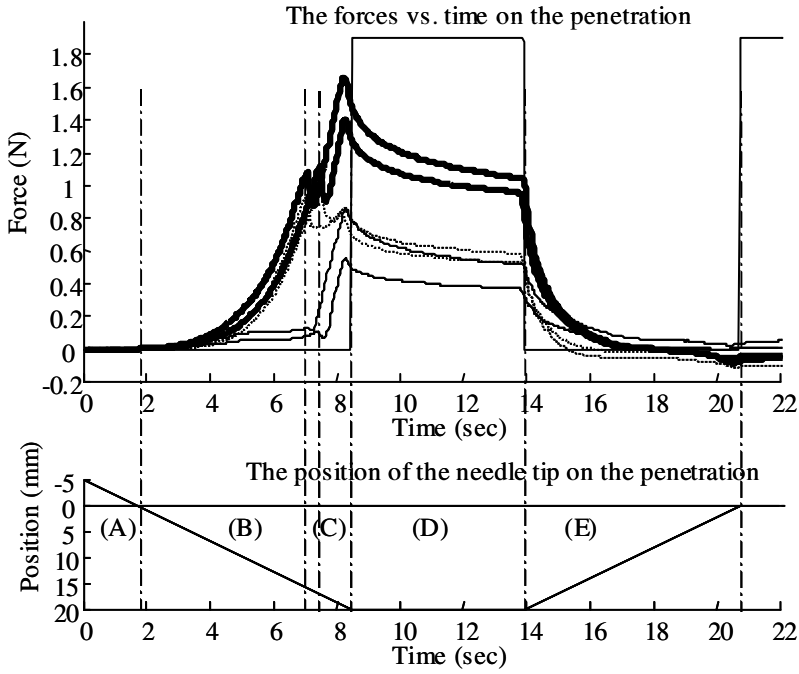

Fig. 5. The total axial, tip and friction forces vs. time together with the trigger signal of the linear stage controller and the position of the needle tip vs. time. The thick line indicates the total axial force, the dotted line the tip force, and the thin line the friction force. The step line indicates the trigger signal, which is high when the needle is stationary. The position of the needle tip is set as 0mm where the surface was before the penetration, and positive in the insertion direction

After the tip touched the prostate surface, the total axial forces increased exponentially and had two peaks. The first peaks were located at 7.2 or 7.5sec. We defined the period following (A) until the first peak as (B). During this period, the tip forces followed the total axial force until the first peak, but the friction forces remained low. The needle tip moved about 16mm during period (B) according to the needle speed. After the first peak the total axial forces decreased about 0.2N, and increased again until the needle stopped. We defined this period as (C). During period (C), the tip forces followed this decrease at the beginning, and remained constant with some noise. In contrast, the friction force increased proportionally to time. We defined the period following (C) until when the needle started to be pulled up as (D). During this period, all of the forces decreased exponentially, and the tip forces remained positive without being zero. The following period until the needle stopped again was defined as (E), where the forces decreased more drastically. The tip forces became negative at the end of (E).

After the whole procedure completed, it was observed that the needle tip was still inside the tissue even when the tip position was at the location of the prostate surface before penetration. At this time, the prostate surface was raised.

In these procedures, needle deflection was not observed on the X-ray monitors, and the transverse force of the needle, which was also measured together with the axial forces, was almost zero. Therefore, we ignore the transverse force in this report.

4 Discussion

Since the tip forces traced the total axial forces during period (B), and the friction forces remained low while they increased during period (C), it is considered that only the needle tip touched to the surface without insertion into the prostate during (B). This means that the first peak revealed the puncture of the prostate surface, and the needle just compressed the surface until the tip force reached the magnitude required for puncturing the surface membrane. Since this magnitude would change due to the shape and sharpness of the needle tip, needle simulators should differentiate the peak value according to the needle tip. The tip forces in (B) increased exponentially. This means that the behavior of the prostate tissue under compression by a point is not linear elastic. It is possible that this characteristic was caused by the non-elasticity of the tissue or the effect of shear stress on the surface membrane. Since the needle penetration into a swine hip muscle without skin revealed the same characteristic in our previous experiment [6], we suppose that the latter hypothesis has higher possibility. Further investigation is required.

The tip forces during period (C) decreased at first. This occurs because the force required to cut the tissue inside the prostate was less than that required to puncture the surface membrane of the prostate. The tip force slightly increased after the decrease. Assuming that the tissue inside the prostate is uniform, it is expected that the tip force remained constant after the decrease. We consider that this increase was caused by the resistance force of the tissue below the prostate against its compression, therefore the increase can be ignored for simulating the reaction of the prostate itself. The linearity of the increase of the friction force in (C) means that the friction force was proportional to the true insertion depth of the needle, since the true insertion depth also increased linearly with time due to the constant speed of the needle. The true insertion depth can be obtained by subtracting the 16mm surface motion of the prostate in (B) from the driving distance of the needle by the linear stage. Assuming that the uniform diameter of the needle generates the uniform clamping force along the axis, it is expected that the distribution of the friction force is also uniform along the axis. The linearity between the friction force and the true insertion depth encourages this assumption. Penetration with needles of different diameters is planned in order to investigate the relation between clamping force and needle diameter. It is expected that the slope of the friction force will increase following the increase of the needle diameter. In a needle simulation, the total axial force in this period will be represented as the sum of the tip force, which decreases at the beginning from the value for the surface puncture to the value for the cutting force of tissue and remain constant, and the friction force, which increases proportionally to the true insertion depth according to the needle diameter.

The decrease of all the forces in (D) is supposed to be caused by the viscosity of the tissue. Since the tip forces were not zero, the needle tip still compressed the tissue even when it did not cut the tissue. The decrease of the friction force was caused by the decrease of the dragging-up force of the tissue edge facing to the needle, not by

the decrease of the contact area on the needle surface to the tissue, because it was observed that the prostate surface did not move during (D) in the X-ray images. Since it is considered that the decrease of both the tip and friction forces were governed by the same viscosity model, the total axial force in the simulation will be also represented by that viscosity model.

During period (E), the needle was drawn out from the tissue, and the tissue was also stretched simultaneously by releasing the compression. Considering that the tip force remained positive in the former part, it is possible that the stretch of the tissue started first, then the drawing of the needle followed, because the drawing of the needle would drastically reduce the force to zero or negative. The decrease of static friction force by the dragging-up force at the tissue edge facing to the needle (an exponential function of time) and the decrease of the dynamic friction force by the drawing of the needle (a linear function of time) occurred simultaneously. Thus, it is difficult to distinguish them. The reason that the tip force remained negative at the end of (E) is that the tissue was still held on the needle and the raised tissue pulled down the needle tip even when the needle at the location of the surface before penetration. For a simulation model in this period, the tip force will decrease exponentially in the same order as in period (B) until it reaches a negative value, which will be determined by the maximum true insertion depth. This depth is determined by the amount of the held tissue on the needle, and the friction force will also decrease, where the same exponential function as the tip force and the linear function for drawing out are added.

5 Conclusions

The tip force and the friction force on a needle during penetration into a canine prostate were independently measured by a newly-developed 7-axis load cell, and each force was related to the mechanical behavior of the prostate tissue. The change of the behavior of friction force during penetration revealed the puncture of the surface, and the true insertion depth of the needle in the tissue was also estimated from the puncture of the surface. The linearity of the friction force during the insertion imply that the friction force was generated uniformly along the axis by the constant clamping force depending on the needle diameter. The tip and friction force when the needle stopped revealed the viscosity of the tissue, and it was suggested that the tissue stretch is prior to the needle drawing when the needle was released. The overview of the needle simulation model was also revealed as the combination of an exponential function and a linear function. Additional experiments with the needles of different diameter and with different true insertion depths will be performed in near future.

Acknowledgement

This work is supported by AIST grant for international collaborative research and National Science Foundation grant ERC 9731748. The authors thank Dr. Rand Brown, DVM and Dr. Gabor Fichtinger for their assistance with experiments.

References

1. Hiemenz, L., Stredney, D., and Schmalbrock, P., "Development of the force-feedback model for an epidural needle insertion simulator," Medicine Meets Virtual Reality 6, pp. 272-277, 1998.
2. Westbrook, J. L., Uncles, D. R., Sitzman, B. T., and Carrie, L. E. S., "Comparison of the Force Requied for Dural Puncture with Different Spinal Needles and Subsequent Leakage of Cerebrospinal Fluid," Anesth Analg, Vol.79, pp.769-72, 1994.
3. Brett, P. N., Harrison, A. J., and Thomas, T. A., "Schemes for the Identification of Tissue Types and Boundaries at the Tool Point for Surgical Needles," IEEE Trans on Info Technol Biomed, Vol.4, No.1, pp.30-36, 2000.
4. Brett, P. N., Parker T. J., Harrison, A. J., Thomas, T. A., and Carr, A., "Simulation of resistance forces acting on surgical needles," Proc. Instn Mech Engrs, Vol. 211, Part H, pp.335-347, 1997.
5. Simone, C. and Okamura, A.M., "Haptic Modeling of Needle Insertion for Robot-Assisted Percutaneous Therapy," Proc. IEEE International Conference on Robotics and Automation, pp. 2085-2091, 2002.
6. Kataoka, H., Washio, T., Chinzei, K., Funamoto, Y., and Mizuhara, K., "Experimental Analysis of Resistance Acting on a Surgical Needle," Proc. NordTrib2002, Stockholm, June, 2002.